
Figures and figure supplements

The role of surface adhesion on the macroscopic wrinkling of biofilms

Steffen Geisel et al

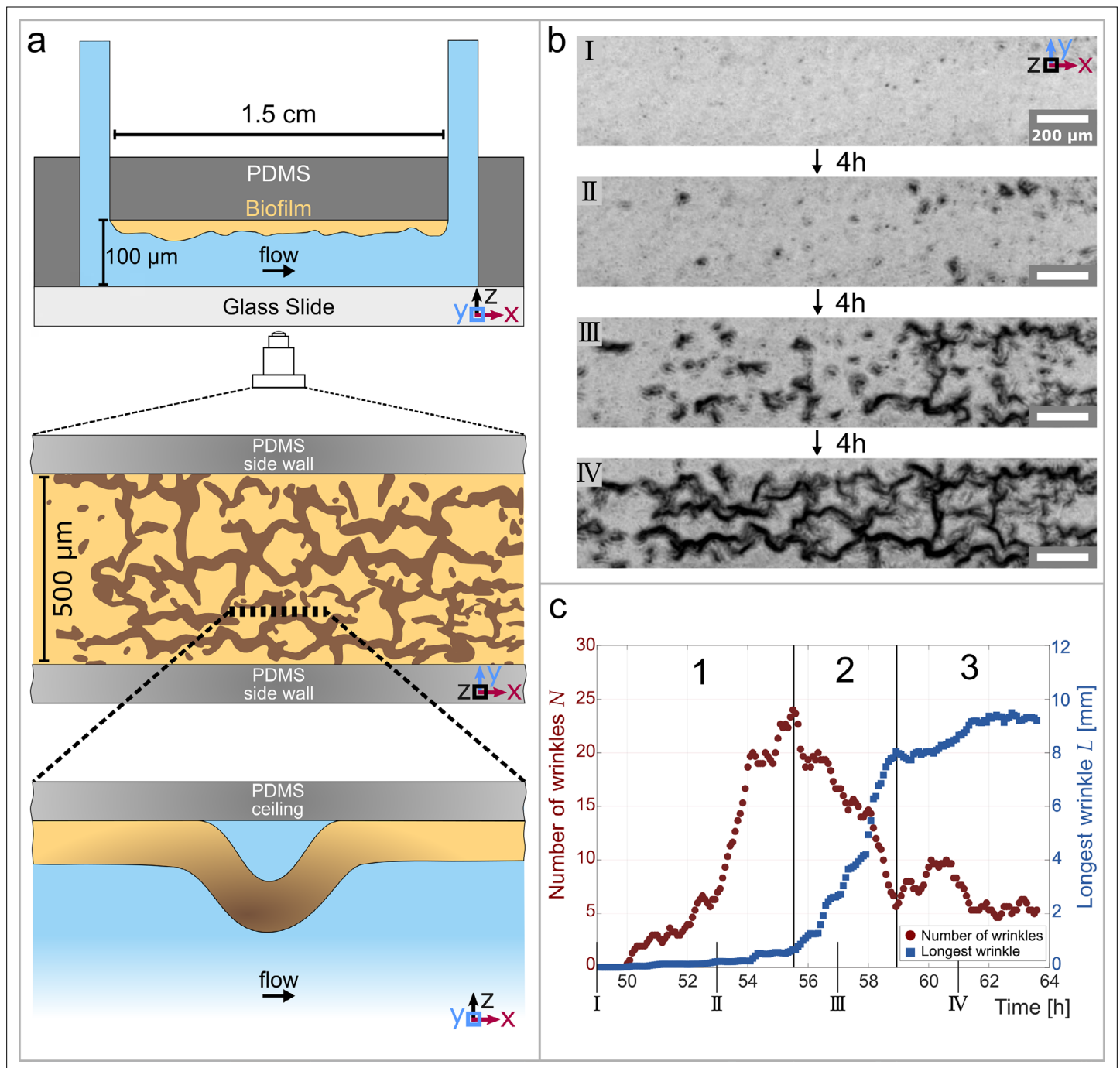


Figure 1. Temporal and structural evolution of wrinkles in *P. aeruginosa* PAO1 biofilms grown in flow. **(a)** Schematic representations of the microfluidic device, the wrinkle network in the biofilm and a side view of a single wrinkle. **(b)** Time evolution of the wrinkled structure in the biofilm. Images were taken in phase contrast. **(c)** Number of individual wrinkles, N (red) and the length of the longest connected wrinkle L (in mm, blue). The evolution of the wrinkled biofilm can be divided into three distinct stages. Many small, isolated wrinkles appear in the first stage. The wrinkles connect to form a network in the second stage. In the third stage, the biofilm has reached a steady state.

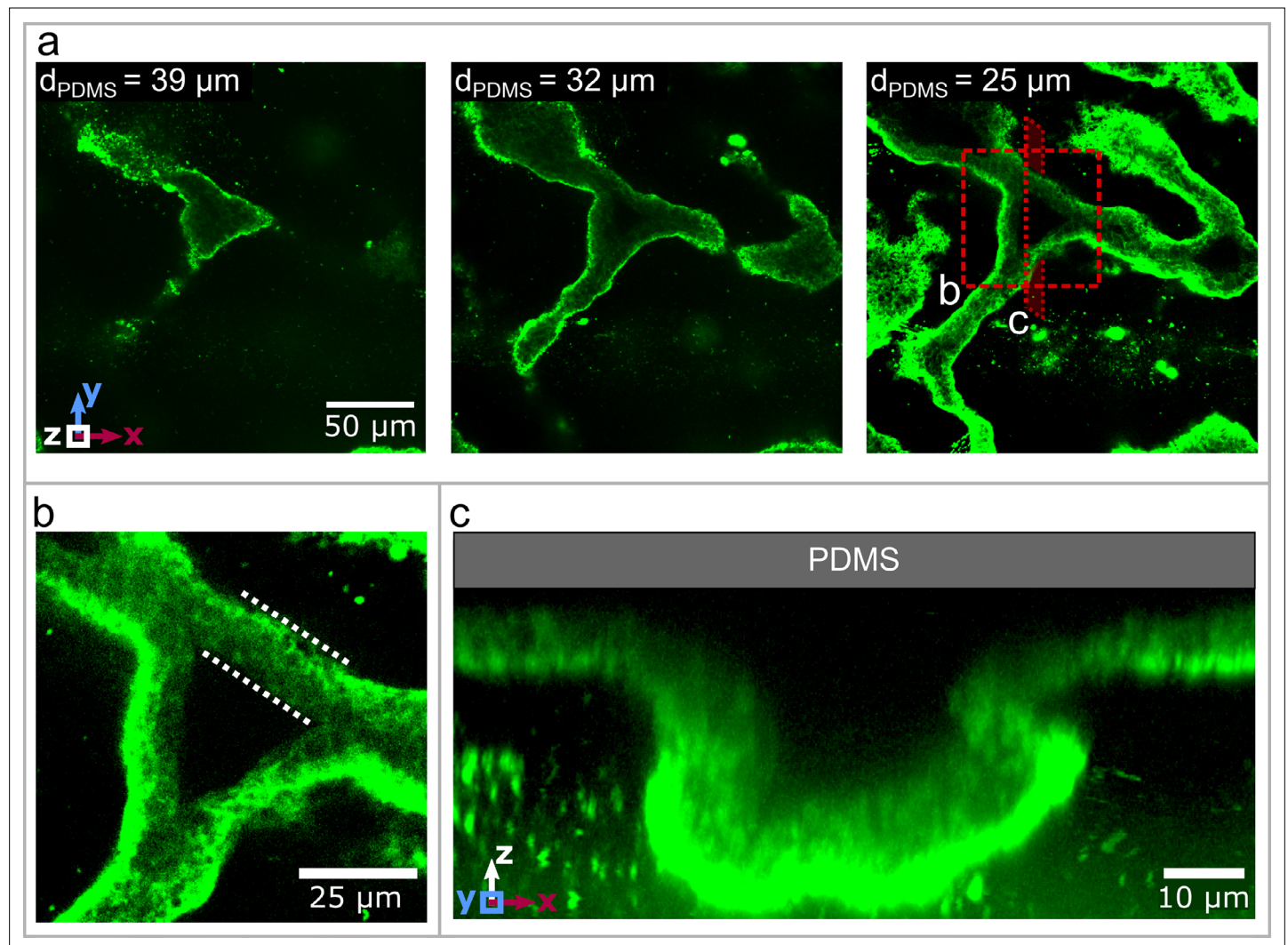


Figure 2. Three dimensional structure of the biofilm wrinkles. (a) Laser-scanning confocal microscopy images of a biofilm that developed a channel network, stained with a GFP-labelled Concanavalin A lectin stain. The three images show slices in the x-y-plane, starting $39 \mu\text{m}$ away from the PDMS surface. The second image is taken $32 \mu\text{m}$ and the third image $25 \mu\text{m}$ away from the PDMS substrate. (b) Close up of the biofilm channel shown in panel (a). The white, dotted lines indicate the walls of the biofilm channel. (c) Cross-section and close up of a channel along the cutting plane indicated in panel (a).

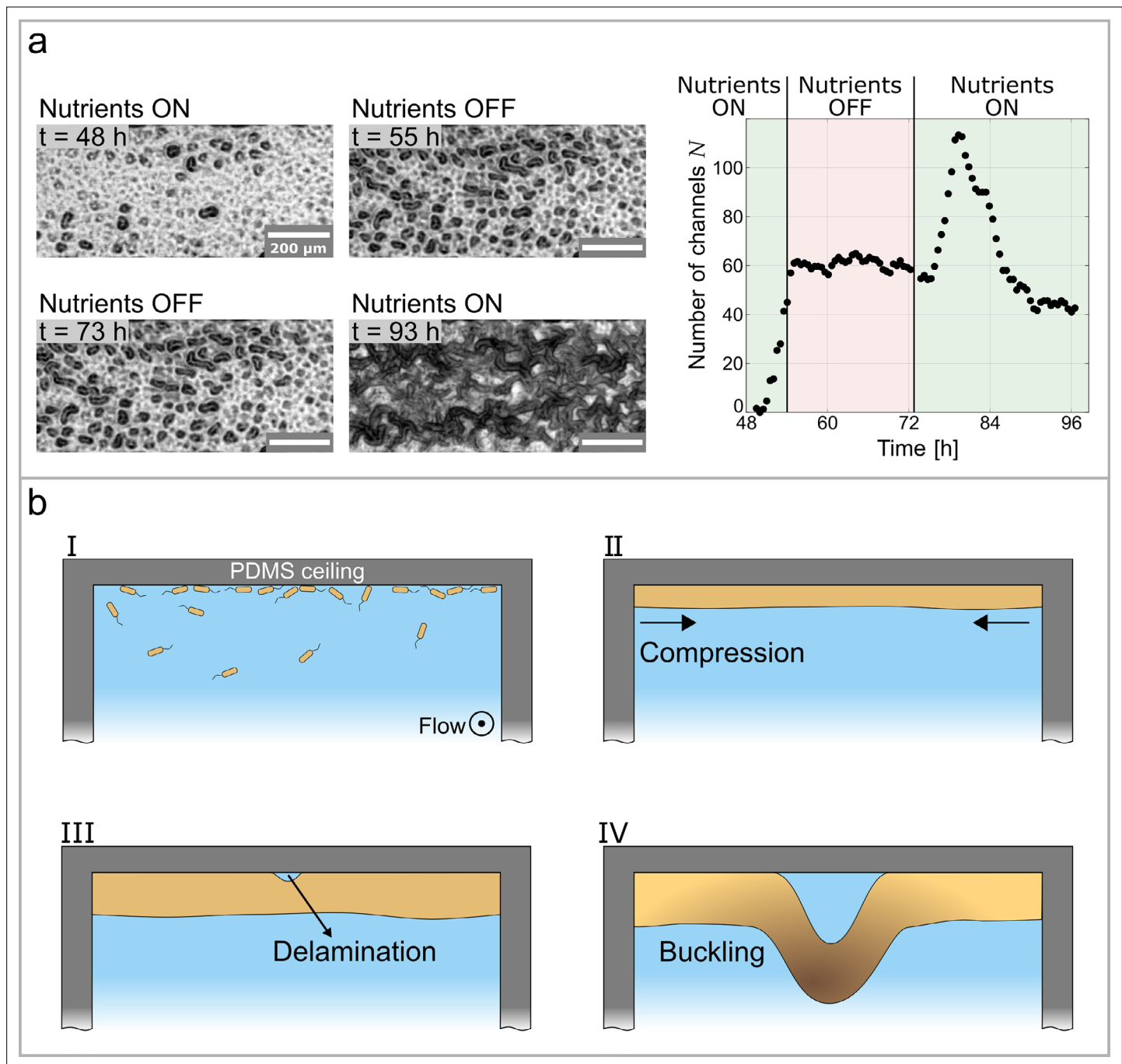


Figure 3. Growth controls the formation of channels through buckling-delamination. **(a)** Phase-contrast images of the experiment conducted to investigate the role of biofilm growth in channel formation. At $t = 55$ h the nutrient solution is replaced with a nutrient-depleted salt solution to stop growth. At $t = 73$ h the salt solution is replaced with the original nutrient solution. The graph shows the number of channels, N , as a function of time and nutrient availability. **(b)** Schematic representation of the buckling-delamination mechanism during channel formation in *P. aeruginosa* biofilm in a microfluidic device.

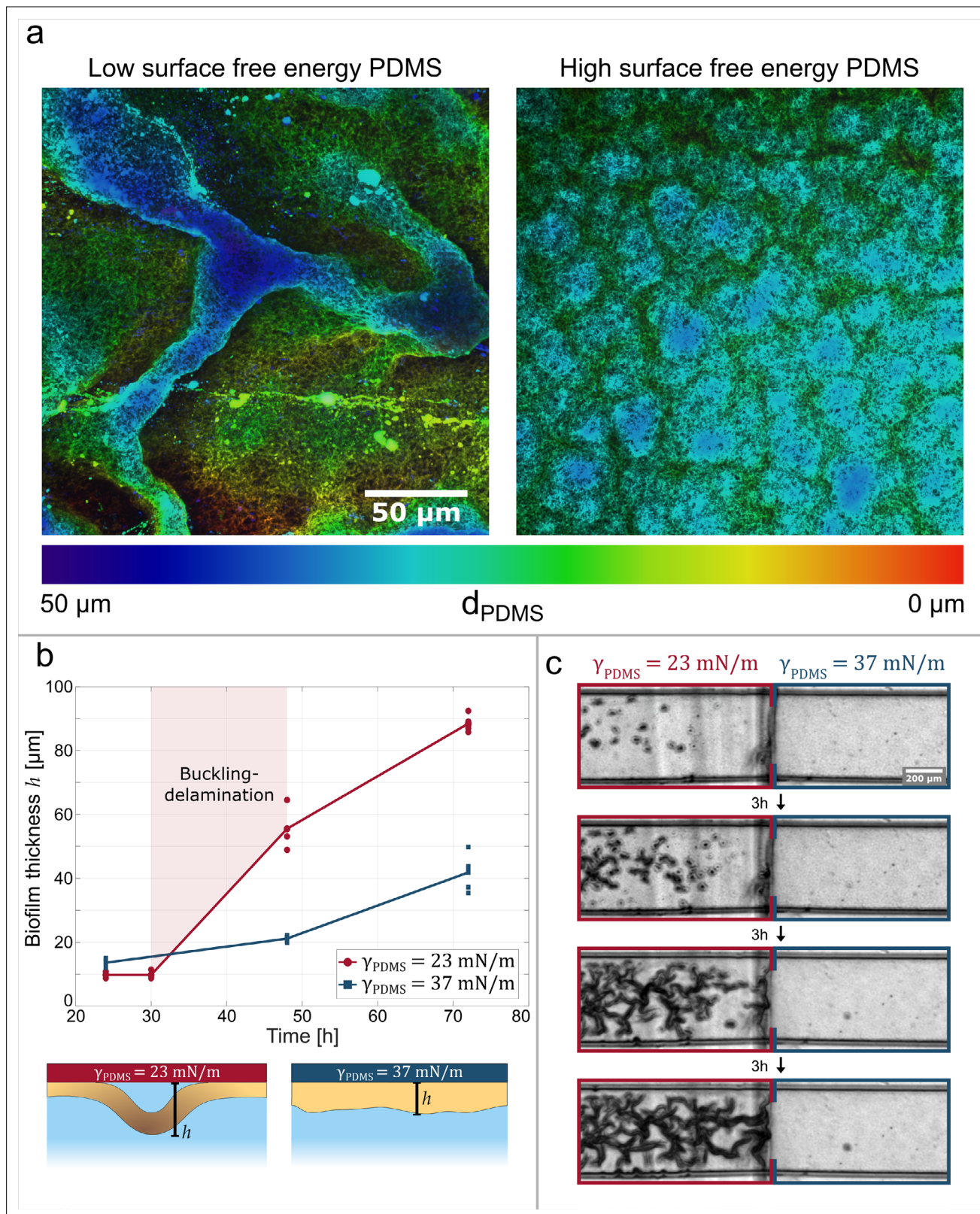


Figure 4. Adhesive strength between the biofilm and the substrate governs channel formation. **(a)** Reconstructions from laser-scanning confocal microscopy images of the biofilm. The biofilms are either grown on a low surface free energy PDMS substrate (left, $\gamma_{\text{PDMS}} = 23 \text{ mN m}^{-1}$) or on a high surface free energy PDMS substrate (right, $\gamma_{\text{PDMS}} = 37 \text{ mN m}^{-1}$). **(b)** Average effective biofilm thickness as a function of time and surface free energy. The average thickness of biofilm grown on a low surface free energy PDMS substrate (red) and on a high surface free energy PDMS substrate (blue).

Figure 4 continued on next page

Figure 4 continued

(c) The image sequence shows a biofilm that is grown on a patterned PDMS substrate in the same microfluidic channel. On the left, the substrate has a low surface free energy, while on the right it has a high surface free energy.

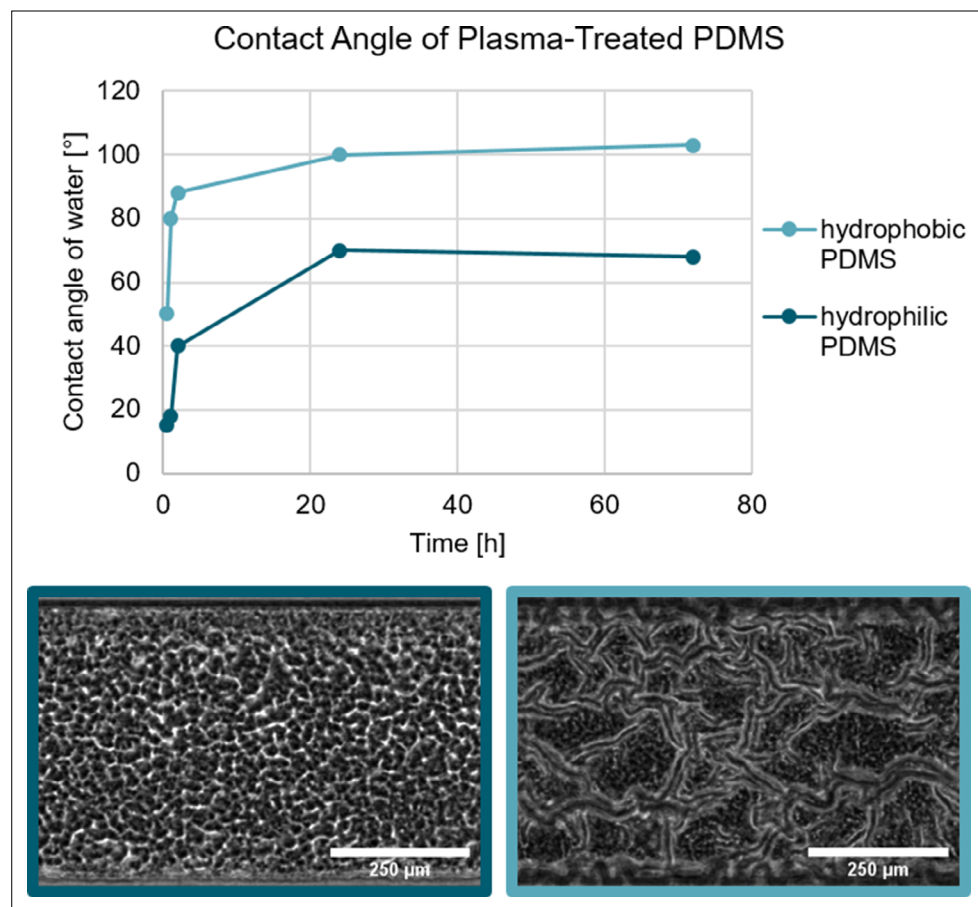


Figure 4—figure supplement 1. The surface free energy of the substrate can be changed through a physical process. The treatment of PDMS with an oxygen plasma increases the hydrophilicity with identical results to the chemical modification. Biofilm growth on hydrophilic and hydrophobic PDMS substrate. In both cases, the PDMS was treated with an oxygen plasma which renders the PDMS hydrophilic. As shown by *Kim et al., 2004* the hydrophobic recovery of plasma-treated can be varied depending on the storage conditions. Biofilm grown on the hydrophilic PDMS does not form a channel network, while the biofilm grown on the hydrophobic PDMS does form a channel network.

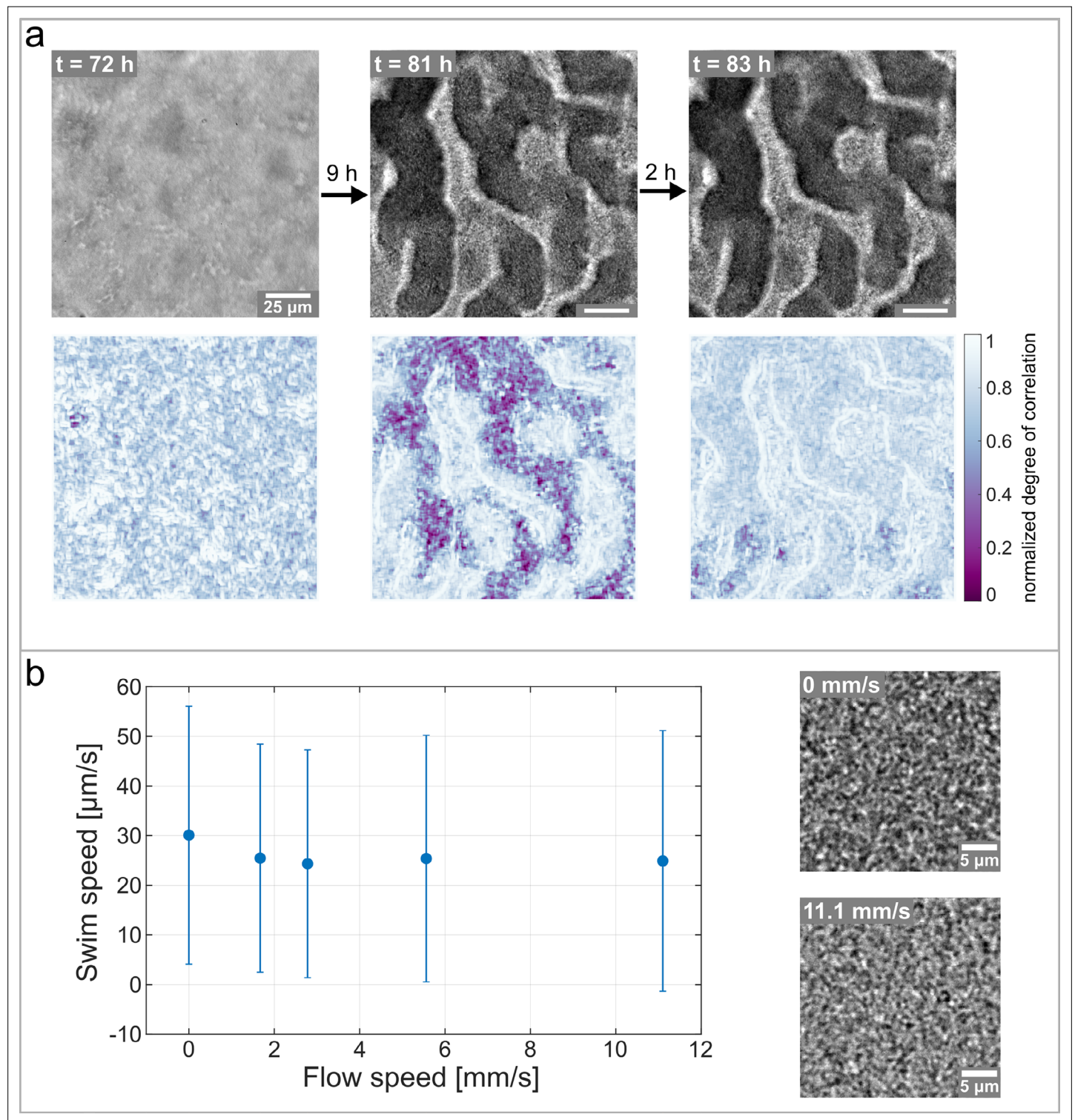


Figure 5. Hollow channels are populated by motile bacteria. **(a)** Bacterial movement inside the channel network visualized using a spatially resolved, normalized degree of correlation. A low degree of correlation corresponds to an active region. The brightfield images show the corresponding structure of the biofilm. **(b)** Differential Dynamic Microscopy is used to quantify the bacterial swimming speed inside the biofilm channels. The swimming speed is measured at varying fluid flow speeds inside the microfluidic device. The two microscopy images show a close up of the bacterial biofilm at two different fluid flow velocities. The errorbars indicate the standard deviation from the mean swim speed. The videos of the bacteria motion can be found in **Figure 5—video 2** and **Figure 5—video 3**.